Physics Letters A 381 (2017) 1405–1410

Contents lists available at ScienceDirect

Physics Letters A

www.elsevier.com/locate/pla

Above-threshold ionization through Rydberg state population

Pei Pei Xin [a,b], Ming Hu Yuan [a,b], Han Mu Wang [a,b], Hai Feng Yang [c], Hong Ping Liu [a,b,*]

[a] State Key Laboratory of Magnetic Resonance and Atomic and Molecular Physics, Wuhan Institute of Physics and Mathematics, Chinese Academy of Sciences, Wuhan 430071, People's Republic of China
[b] University of Chinese Academy of Sciences, Beijing 100049, People's Republic of China
[c] College of Physics and Electronic Information, Luoyang Normal University, Luoyang 471022, People's Republic of China

ARTICLE INFO

Article history:
Received 22 December 2016
Received in revised form 14 February 2017
Accepted 20 February 2017
Available online 28 February 2017
Communicated by V.A. Markel

Keywords:
Above-threshold ionization
Rydberg state population
Atomic core potential

ABSTRACT

We present a theoretical scenario for the atomic above-threshold ionization (ATI) in an intense laser field by investigating the Rydberg state population in real time. Rather than merely viewing the final distribution of photoelectron yield directly, we monitor the Rydberg state population by projecting the time-dependent wave function onto the bound eigen-states. The calculation shows that the population of resonant Rydberg states is closely related to the peaks in photoelectron kinetic energy spectrum (PKES). For a hydrogen atom, the highest populated Rydberg states are degenerated, exactly corresponding to the first ATI peak if one additional photon is absorbed. While for non-hydrogen atoms, e.g., Ar, the highest Rydberg states are mainly populated on specific states, e.g., $3d(5s)$ and $4f$ in our case, also giving exact peak positions in PKES, where the state identification is obtained by the angular momentum resolved distribution of excited Rydberg states. This method provides an easy to understand picture for the resonance-enhanced effects in ATI as well as the role of atomic core potential in strong-field ionization.

1. Introduction

Increasingly shorter pulses with duration of the order of (sub)-femto to attoseconds make it possible to study the interaction of few-cycle pulses with atoms or molecules [1]. It is widely perceived that an electron can be ionized through either a multiphoton or a tunneling mechanism, depending on the value of the Keldysh parameter $\gamma = \sqrt{I_p/(2U_p)}$ [2], where I_p is the ionization potential of the target atom and U_p is the ponderomotive energy. In the multiphoton regime ($\gamma > 1$), an electron can absorb more photons than necessary to overcome the ionization potential, which is called above-threshold ionization (ATI) [3–5]. Therefore, the resulting energy spectra show regular ATI peaks separated by one photon energy. At the same time, all peaks are shifted by the ponderomotive potential.

Due to the transient resonances of ac Stark-shifted Rydberg states, the low order ATI peaks can break up into substructures, which is called Freeman resonance [6]. A radial pattern with a shape of a bouquet near and below the first ATI order has been observed experimentally [7,8] and theoretically [9,10]. It is considered that such distribution in the near-threshold continuum results from the interplay between different electron trajectories in the laser and the Coulomb fields, which is also concluded by introducing a variable cut-off function to make a number of different long-range potentials [11,12].

More extensive study in this energy range is via the simultaneous measurement of the photoelectron kinetic energy spectrum (PKES) and photoelectron angular distributions (PADs) [13–15]. This combined technique observes jet structures which correspond to angular momenta of the resonant Rydberg state in the PADs of low-order ATI peaks and ring structures in the PADs of high-order ATI peaks, respectively. Considering the long-range Coulomb potential, Chen et al. [11] further established an empirical rule that the dominant angular momenta of the low-energy photoelectrons are related to the initial state and the minimum number N of absorbed photons to reach the continuum. However, no clear physical interpretation of these dominant angular momenta was provided there. A widely accepted interpretation was reported by Arbó et al. [9], who attributed the Ramsauer–Townsend-type diffraction oscillations in the angular distribution to being the nature properties of the interfering classical trajectories in the presence of both the Coulomb and laser fields. This interpretation was then confirmed experimentally by Marchenko et al. [16,17], who showed that there are two major contributions arising from the interference in the momentum spectra, and the resonant substructures in the energy spectrum could be influenced by the presence of non-resonant ionization.

* Corresponding author.
E-mail address: liuhongping@wipm.ac.cn (H.P. Liu).

http://dx.doi.org/10.1016/j.physleta.2017.02.035
0375-9601/

In this paper, rather than merely viewing the final distribution of photoelectron yields directly, we monitor the bound Rydberg state population in real time. Our calculation is carried out for hydrogen atom H and non-hydrogen atom Ar from the tunneling regime to the multiphoton regime, where the information of Rydberg state population is obtained by projecting the time-dependent wave function onto the bound states. The correlation of the bound intermediate Rydberg state population with the photoelectron kinetic and angular momentum distribution provides a different angle to understand the multiphoton ionization in low-energy range, as well as the population trapping of Rydberg states in ionization [18] and surviving of Rydberg states in photoionization [19,20].

2. Theoretical method

The time-dependent Schrödinger equation (TDSE) for an electron under the influence of a classical electromagnetic field in atomic units reads:

$$i\frac{\partial}{\partial t}\psi(\mathbf{r},t) = H(\mathbf{r},t)\psi(\mathbf{r},t). \tag{1}$$

Here the Hamiltonian of an atom interacting with a linearly polarized laser field within the single electron approximation is:

$$H(\mathbf{r},t) = \frac{\mathbf{p}^2}{2} + V(\mathbf{r}) + \mathbf{r}\cdot\mathbf{F}(t), \tag{2}$$

where $\mathbf{p}$ and $\mathbf{r}$ are the momentum and position of the electron, respectively, $V(\mathbf{r})$ is the atomic central potential, and $\mathbf{F}(t)$ is the time dependent external electric field.

In this work, we use the effective atomic potential which is parameterized by [21]

$$V(\mathbf{r}) = -\frac{Z + a_1 e^{-a_2 r} + a_3 r e^{-a_4 r} + a_5 e^{-a_6 r}}{r}, \tag{3}$$

where Z is the charge of the residual ion and the parameters a_i are obtained by fitting the numerical potential calculated from the self-interaction free density functional theory [22]. The laser pulse is chosen to be of the form:

$$\mathbf{F}(t) = F_0 \sin^2(\frac{\pi t}{\tau})\cos(\omega t + \varphi)\hat{Z};\ (0 \le t \le \tau), \tag{4}$$

where ω is the laser carrier frequency, φ the carrier-envelope phase, τ the total pulse duration, F_0 the peak field, and $\hat{Z}$ the polarization direction.

In the numerical calculations, $\psi(\mathbf{r},t)$ is expanded as

$$\psi(\mathbf{r};t) = \psi(r,\theta,\phi;t) = \sum_l \frac{R_l(r;t)}{r} Y_{lm}(\theta,\phi), \tag{5}$$

where the angular part is expanded with the spherical harmonics for a fixed magnetic quantum number m. The radial part $R_l(r;t)$ of the wavefunction is expanded in the discrete variable representation (DVR) basis [23–26]. The wavepacket propagation is performed by using the split-operator method [26]. We calculate the probability of the electron on the bound state by projecting $\psi(\mathbf{r};t)$ onto the corresponding field-free eigenstates $\psi_{nlm}(\mathbf{r})$,

$$P_{nlm} = |\langle\psi_{nlm}(\mathbf{r}) \mid \psi(\mathbf{r};t)\rangle|^2. \tag{6}$$

The probability of the electron on the Rydberg state n is $P_n = \sum_{lm} P_{nlm}$. The total ionization probability is given by

$$P_{ion}(t) = 1 - \sum_{E_{nlm}<0} |\langle\psi_{nlm}(\mathbf{r}) \mid \psi(\mathbf{r};t)\rangle|^2. \tag{7}$$

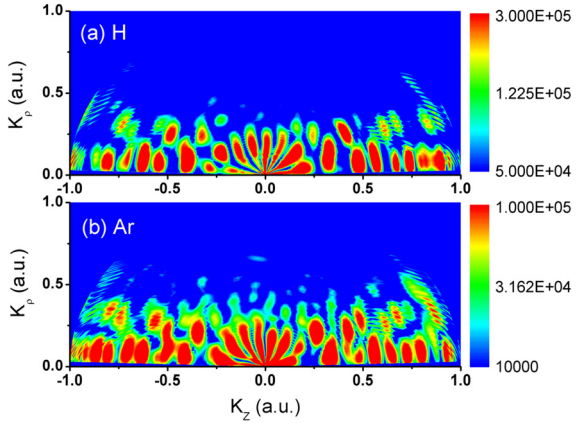

Fig. 1. (Color online.) Calculated photoelectron momentum distributions for H and Ar in tunneling ionization region for a 800 nm, 1.7×10^{14} W/cm^2 laser pulse.

The calculation of the 2D momentum distribution requires projection of the wave function $|\psi(\mathbf{r};t)\rangle$ after the laser pulse vanishes onto the outgoing continuum functions [27,28]

$$\frac{dP}{d\mathbf{k}} = \frac{1}{4\pi k}\left|\sum_l e^{i\delta_l(k)}\sqrt{2l+1}\,P_l(\cos\theta)\,\langle k,l \mid \psi(\mathbf{r};t)\rangle\right|^2, \tag{8}$$

where $\delta_l(k)$ is the momentum-dependent atomic phase shift, θ is the angle between the electron momentum k and the polarization direction of the laser field $\hat{Z}$, P_l is the Legendre polynomial of degree l, and the partial wave $|k,l\rangle$ is the eigenstate of the atomic Hamiltonian with positive eigen-energy $E = k^2/2$ for orbital quantum number l. Note that in Eq. (8), only $m = 0$ is taken into account for atom H with initial s state. It is also applicable for atom Ar in a linearly polarized laser pulse, even though the atom is initially in the p state. We omit the contribution of the ionization probability from $m = \pm 1$ since they are much smaller in comparison to the $m = 0$ component.

3. Results and discussion

Before studying the atomic multiphoton ionization dynamics, we'd like to have a brief view of the main features of its tunneling ionization favored by small Keldysh parameters ($\gamma < 1$), e.g., for atom H and non-hydrogen atom Ar. In this strong field region, the ionization dynamic behavior shows a similarity even for different atomic species. A typical laser pulse of peak electric field 1.7×10^{14} W/cm^2 is used in the calculation with its wavelength 800 nm, total duration 18 fs, comprising 6 cycles.

In Fig. 1 we present the two-dimensional momentum distributions for photoionization of H and Ar atoms in this tunneling ionization region. First of all, we can notice the similarity of the doubly differential momentum distributions for the two different atomic targets. The interference patterns are characterized by a transition from a ring-shaped pattern at larger k with circular nodal lines to a pattern of pronounced radial nodal lines for small k near-threshold resembling experimental results [7,8]. The circular nodal structure reflects the dominant angular momentum and parity of the photoelectrons at the constant energy [9,13]. Furthermore, within the first ATI peak, the bouquet shaped structures have been found to be the major features resulting from the interplay between different electron trajectories in the combined laser and Coulomb fields [9]. Both atoms have close ionization potentials (hydrogen $I_p = 13.6$ eV and argon $I_p = 15.76$ eV) and therefore their photoelectron momentum distributions show radial jets with the same numbers, which depends on the binding energy and the laser intensity [29].